

A MODEL TO EXPLAIN THE CORRELATION BETWEEN THE OPTICAL AND RADIO
PROPERTIES OF HIGH-REDSHIFT GALAXIES

R. A. DALY

Joseph Henry Laboratories, Princeton University
Received 1988 December 9; accepted 1989 December 6

ABSTRACT

Recent observations indicate that steep-spectrum radio sources are often galaxies at high redshift which have optical and near-infrared continuum emission originating from a region which is elongated, and the axis of this elongation is the same as that defined by the radio lobes, as discussed by Chambers *et al.* and McCarthy *et al.* Such a correlation between the optical and radio axes could arise if the optical and infrared emission were the end result of the action of jets tunneling through the ambient gas associated with the galaxy/protogalaxy. As detailed here, the action of jets tunneling through an ambient medium leads to two coupled shock systems: a driven shock wave along the jet axis and a blast wave perpendicular to the jet axis. Hence, the action of jets tunneling through the ambient protogalactic medium sends a shock wave perpendicular to the radio jet axis; this not only shock heats the ambient gas, but it also, under appropriate conditions, triggers star formation. The optical and infrared emission could arise from the stars and/or from the shock-heated gas, and because the envelope of the blast wave is elongated along the axis defined by the jets, the optical emission will arise from a region whose elongation axis is the same as that of the jets. The radio emission arises from the radio lobes which are inferred to be the termination regions of the jets, where the action of the jet tunneling through the ambient medium is taking place. Such a model for the “alignment effect” leads to several consequences. The power being channeled into the jets, the relative extent of the emitting regions, the conditions necessary for star formation to occur, the relation between the spatial extent of the red and blue continuum components and the emission-line region, how long the alignment will persist, the implications for the epochs of galaxy formation, and the implications for the immediate environment of these galaxies are discussed.

Subject headings: galaxies: jets — galaxies: evolution — hydrodynamics — radio sources: galaxies — shock waves

I. INTRODUCTION

Steep-spectrum radio galaxies are often at high redshift ($z \gtrsim 1$) and have optical emission originating from a region which appears to be elongated, where the elongation axis is close to that defined by the positions of the radio lobes (Chambers, Miley, and van Breugel 1987, 1988; McCarthy *et al.* 1987b). Typically, the projected separation between the radio lobes is greater than the projected length of the optically emitting region, and the region of optical emission is roughly centered between the radio lobes. One associates the optical emission with the galactic/protogalactic material and the radio emission with the termination of the jets in the medium at the extremities of the galaxy or in the intergalactic medium (as discussed, for example, by Begelman, Blandford, and Rees 1984). Clearly, the jets had to tunnel through any ambient gas which was associated with the galaxy/protogalaxy at the time the jets were initially activated. Such interactions are observed: the case of 4C 29.30, discussed in detail by van Breugel *et al.* (1986), is an excellent example of a jet-medium interaction.

Observations of galaxies which exhibit the “alignment effect” suggest that the optical emission results from the jet-medium interaction (Chambers, Miley, and van Breugel 1987; McCarthy *et al.* 1987b). Here the shock systems which will be established as jets tunnel through the ambient medium, and how these may lead to the alignment of the axes defined by the region of optical, infrared, and radio emission, referred to as the “alignment effect,” are described, as are several consequences of this model.

The radio sources selected by Chambers, Miley, and van Breugel (1987) on the basis of their very steep spectrum (spectral index greater than 1) and observed in the optical, were typically found to be high-redshift radio galaxies which exhibit the unexpected properties mentioned above. It is of interest to study the potential causes of the alignment effect and its implications for the epoch of formation, and the evolutionary stages of these galaxies.

It is possible that the alignment is signaling the existence of a galactic evolutionary phase which was previously unidentified, and that most galaxies, or most galaxies of a particular type, undergo a phase of this type. This is suggested by the results of the deep VLA survey of Donnelly, Partridge, and Windhorst (1987). They report observing six objects in their complete 6 cm map (which covers an area of about 450 arcmin²) with a spectral index (50 to 21 cm) steeper than 1, indicating that sources of this type have a surface density of at least 50 objects per square degree (roughly a factor of 10⁴ greater than the surface density of objects of this type reported by Chambers, Miley, and van Breugel 1987, and McCarthy *et al.* 1987b). These sources have 50 cm (608.5 MHz) fluxes ranging from 2 to 8 mJy, and they are unidentified optically. Donnelly, Partridge, and Windhorst (1987) discuss the evidence which suggests that these sources are at redshifts greater than 0.5. If when observed optically, these sources exhibit the “alignment effect” between the radio and optical axes as seen in the sample observed by Chambers, Miley, and van Breugel (1987, 1988), whose selection criterion was a radio spectral index greater than 1, then

such an evolutionary stage may be a not uncommon phase of galactic evolution.

Of course, the signature of the phase and the magnitude of the parameters (e.g., radio luminosity, optical luminosity, radio spectral index, elongation and extent of the region of star formation, etc.) may vary systematically. This is because the "alignment effect" will depend on the power channeled into the jets, the properties of the ambient protogalactic/galactic medium, and on the environment of the galaxy, that is, whether the intergalactic medium surrounding the galaxy is of high or low density. Galaxies in a high-density environment, such as a protocluster or cluster of galaxies, will remain in the "tunneling phase" for a longer period of time because the interaction with the ambient medium will continue out to larger galactic radii, and hence the radio emission will persist for a longer period of time (this is discussed in more detail below, and in § IVg).

On the observational side, the ultra-steep-spectrum radio sources seem to have a fairly constant monochromatic radio luminosity (Chambers, Miley, and van Breugel 1988), and a correlation between the star formation activity and the radio spectral index, and the lack of a correlation between the radio luminosity and the star formation activity for radio sources with a broad range of spectral indices, are discussed by Lilly (1989): these correlations may or may not change as fainter objects are observed. In the context of the model, systematic differences could arise, since the effects of the jets tunneling through the medium are related to the properties of the medium and to the power being channeled into the jets: the properties of the protogalactic medium (and hence the outcome of the tunneling of the jets through the medium) may vary systematically with the power being channeled through the jets, as will be the case if the power being channeled through the jets is related to the mass of the central compact object, which in turn may be related to the density of the protogalactic medium. Also, whether or not star formation is triggered will depend on the properties of the ambient medium and on the properties of the jet (as discussed in § IVd).

In addition to the observations discussed above, several radio sources are now recognized as exhibiting the "alignment effect": 0902 + 34 (Lilly 1988); 4C 40.36 (Chambers, Miley, and van Breugel 1988); 3C 324 (Spinrad and Djorgovski 1984a); 3C 326.1 (McCarthy *et al.* 1987a); the prevalence of strong, extended O II emission with a considerable velocity amplitude amongst a sample of faint 3CR galaxies is discussed by Spinrad and Djorgovski (1984b); Djorgovski *et al.* (1987) discuss the tendency for 3CR galaxies to be elongated, asymmetric, or multinodal; 3C 368 has been investigated in great detail by Djorgovski *et al.* (1987) and by Chambers, Miley, and Joyce (1988); also see LeFèvre and Hammer (1988).

If the alignment effect results from a jet-medium interaction, an organized velocity field is expected: the observed velocity field will be extremely telling. The field can be separated into two components, that along the jet and that perpendicular to the jet. The magnitudes of the velocity gradient in each direction and the spatial extent of the component used to trace the velocity field can be directly linked to the parameters of the model. Observations of an organized velocity field have been noted for 3C 324 (Spinrad and Djorgovski 1984a), for the sample in general, and for the particular source 3C 280 (McCarthy *et al.* 1987b), 3C 326.1 (McCarthy *et al.* 1987a), and 3C 368 (Djorgovski *et al.* 1987); undoubtedly there are other cases. These organized velocity fields support the notion that

the ambient medium is significantly and systematically perturbed by the tunneling of the jets through the medium.

It should be noted that if this is a brief phase of galactic evolution lasting a fraction f of the Hubble time at the redshift of the object, then only a fraction f of all galaxies at that redshift which are undergoing a phase of this type will be observable. Similarly, the probability P of observing a particular galaxy in any given phase is proportional to the time t the galaxy spends in that phase: $P = t/t_H(z)$, where $t_H(z)$ is the Hubble time at the redshift of the galaxy. Clearly, the time a galaxy is in this state depends not only on the properties of the jets and on the ambient medium of the galaxy, but also on its immediate environment: galaxies in regions where the intergalactic medium is of high density (such as a cluster of protocluster of galaxies) will remain in this phase for a longer period of time (i.e., will be a radio source for a longer period of time) and hence will have a higher probability of being detected.

The interpretation of the observations of radio galaxies could be instrumental in constraining the epoch(s) of galaxy formation (e.g., Spinrad 1986; Lilly and Longair 1984; Lilly 1989). In addition to the blue stellar population, indicative of a recent burst of star formation, these objects exhibit red continuum emission indicative of a red stellar population (e.g., Chambers, Miley and Joyce 1988; Lilly 1988, 1989). The epoch of the formation of galaxies exhibiting the alignment effect may be inferred from the color and physical extent of the regions of emission; hence, through this effect, the epoch of the formation of this component may be constrained (see the discussion in § IVf).

The general picture is based upon the assumption that the action of the jets tunneling through a galactic/protogalactic medium affects the gas via shock heating, and may trigger star formation, since this would explain the alignment of the elongated region of optical emission with the axis defined by the positions of the radio lobes; this general picture is described in § II. Analytic expressions describing the shock systems which will form as the jets tunnel through an ambient medium with a specified density profile are presented in § III. Order of magnitude estimates of relations between several parameters which describe the properties of a system may be obtained from these expressions. The relations are applied and discussed in § IV; the contents of each subsection are described in the opening paragraphs of that section. The model and its implications are summarized in § V.

II. THE GENERAL PICTURE

As described above, optical emission from high-redshift, steep-spectrum radio galaxies originates from a region roughly elliptical in shape with an elongation axis along that defined by the positions of the radio lobes. The radio lobes are inferred to be the termination regions of material flowing through well-collimated jets, assumed to originate from a central compact object located roughly midway between the two radio lobes, which in general is close to the center of the region of optical emission. Clearly, in order to have carved a channel, a jet must tunnel through any ambient gas in its path; indeed, the radio lobes are in all likelihood the interface between the jets and ambient (intergalactic or galactic) material (e.g., Begelman, Blandford, and Rees 1984). The claim is that the action of the jets tunneling through the ambient gas shock heats the gas and may trigger star formation, and that the region affected is elongated in shape with an axis along that defined by the radio lobes.

Reduced to its barest essentials, the model is based upon two assumptions, which seem to be well substantiated by observations. First, it is assumed that a compact source is embedded in the center of a roughly spherical gas cloud (a galaxy or protogalaxy). Second, it is assumed that the compact source is ejecting material at supersonic velocities (relative to the sound speed of the ambient medium and to that of the plasma in the jet) along two well-collimated, oppositely directed jets. These two assumptions are sufficient to determine the shock systems which will form as the jets tunnel through the ambient gas.

When a jet impacts the ambient material in its path, the gas will be shock heated and accelerated; the postshock temperature and velocity may be obtained from the shock jump conditions. The velocity is necessarily less than that of the material flowing through the jets. Because the flow within the jets is assumed to be supersonic, a second shock region along the jet axis will form as the material flowing through the jet rams into the shocked ambient gas. That is, a driven shock wave will form, its geometry being cylindrically symmetric. This situation is very similar to that studied in great detail by Parker (1963), Hundhausen (1985), Chevalier and Imamura (1983), and others for the solar and stellar winds, except that spherical symmetry is now replaced by cylindrical symmetry. As shown in Figure 1, the driven shock wave along the symmetry axis of the jet has two shocked regions, separated by a contact discontinuity (boundary 4). The outer shock (labeled OS) contains the shocked ambient gas, and the inner shock

(labeled IS) contains the shocked jet material. Initially, the velocity of the shocked ambient gas in the outer shock is in the direction of the jet axis, and the pressure is isotropic in the rest frame of the fluid. Therefore, there will be a pressure discontinuity across boundary 2 which separates the shocked ambient gas from the adjacent ambient gas. This discontinuity causes a blast wave to form. In the rest frame of the outer shock, the blast wave will be principally directed perpendicular to the symmetry axis of the jet. As the blast wave propagates into the medium shock heating and accelerating the gas, it loses energy and slows down, eventually becoming a sound wave. The region which has been shock heated by the blast wave lies within the shock envelope, and the shock envelope extends to a maximum distance, S_{\max} , perpendicular to the jet axis. Emission resulting from the action of the jets tunneling through the ambient gas will arise from within the shock envelope, with perpendicular distances from the jet axis less than S_{\max} . Whether star formation is triggered as the blast wave propagates into the ambient protogalactic/galactic medium depends on the properties of the jet and on those of the medium prior to the passage of the blast wave, as discussed in detail in § IVd. If the medium is in two phases, that is, cold clouds embedded in hot gas, star formation may be triggered in the cold clouds as the blast wave shocks the "warm" ambient gas (Rees 1989), and the gas which is not condensed into stars will produce free-free and line emission; the high-density gas will be able to cool efficiently and hence could cool to temperatures where

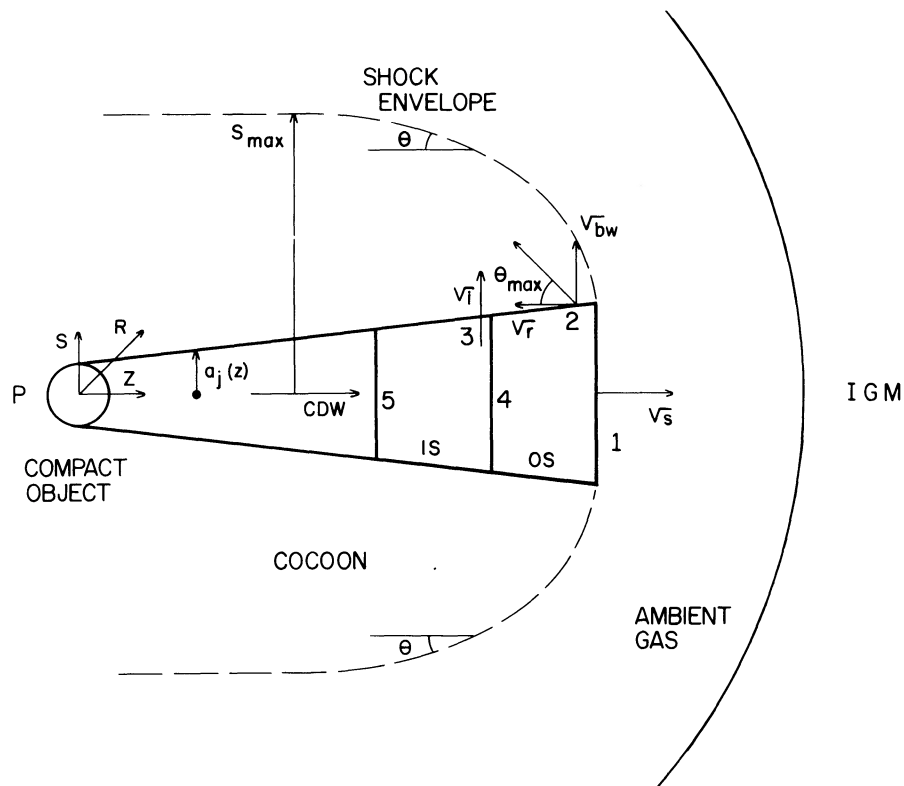


FIG. 1.—Shock systems which form as the jets tunnel through the protogalactic or galactic medium. The collimated driver wind (CDW) is moving supersonically and is shock heated when it encounters the inner shock (IS) boundary (boundary 5). The forward shock front (boundary 1) is moving with a velocity v_s . Pressure equilibrium is maintained across the contact discontinuity (boundary 4), which separates the shocked ambient gas (in the outer shock) from the shocked collimated driver wind (in the inner shock). In the rest frame of the forward shock front (boundary 1), the gas in the outer shock (OS) is moving toward the compact object with a (relative) velocity v_r . The blast (or pressure) wave propagates into the ambient gas with a velocity v_{bw} and results from the pressure discontinuity across boundary 2. The pressure gradient across boundary 3 causes shocked jet material to flow into the cocoon with a velocity v_j . The jet is assumed to be cylindrically symmetric; the z-axis is parallel to the symmetry axis of the jet, and the s-axis is perpendicular to the z axis. The term $a_j(z)$ is the cross sectional radius of the jet at the position z.

line emission is important, and, because this material is entrained in the hot gas, the line-emitting gas may have a considerable velocity. The postshock temperature and hence pressure behind the blast wave decreases as the blast wave propagates, which could change the properties of the free-free and line emission as a function of perpendicular distance from the jet axis, and this may change the efficiency of star formation in the cold clouds. If the medium is not in two phases, then star formation may result due to cooling behind the blast wave; this case is studied numerically by De Young (1989). As described in § IVd, a special combination of parameters is required in order for star formation to result due to cooling behind the blast wave; still, it is possible that this mechanism is operating in some sources. Again, as the blast wave propagates away from the jet axis it loses energy and slows down, causing a decrease in the postshock temperature; hence the properties of the shock-heated gas and efficiency of star formation will change with distance from the jet axis.

It should be noted that rotation may be neglected during the tunneling phase if the system possesses little angular momentum or if the velocity of the forward shock front is $\gtrsim 5 \times 10^3$ km s⁻¹ since, in this case, the time scale for rotation is much larger than other relevant time scales in the problem, as discussed in § IVa.

III. CALCULATIONS

Shock waves are discussed in detail by Parker (1963), Hundhausen (1985), and Chevalier and Imamura (1983), to name a few. We are interested in two coupled shock systems: one cylindrically symmetric driven shock wave and the blast (or pressure) wave resulting from the pressure discontinuity set up between the outer shock front of the driven shock wave and the adjacent ambient gas. In these calculations, cooling has been neglected. The manner in which cooling affects these calculations, and the implications for star formation in these systems, is discussed in detail in § IVd.

The fundamental quantities we seek (all of which are illustrated in Fig. 1) are the velocity of the forward shock front, v_s , the velocity of the blast wave, v_{bw} , the angle θ between the blast-wave envelope and the z -axis (the symmetry axis of the jet), the maximum distance of the blast wave from the symmetry axis of the jet, S_{max} , and the relation between the power P emanating from the central compact object and the velocity of the forward shock front. These quantities may be deduced directly as described by Hundhausen (1985) from general considerations which may be applied to any shock front. A shock front sweeps up mass at a rate

$$\frac{dM}{dt} = v_{sf}(R_s) A_s \rho_A(R_s), \quad (1)$$

where R_s is the radial coordinate on the shock front, $v_{sf}(R_s)$ is the velocity of the shock front, A_s is the area of the shock front, and $\rho_A(R_s)$ is the ambient gas density at the shock front. The velocity of the shock front may be written $v_{sf} = dR_s/dt$. Since $dM/dt = (dM/dR_s)(dR_s/dt) = v_{sf} dM/dR_s$, equation (1) becomes

$$\frac{dM}{dR_s} = A_s \rho_A(R_s). \quad (2)$$

Again following Hundhausen (1985) and Parker (1963), the total energy, W , in the shock wave may be written

$$W = \int (0.5 \rho v^2 + 1.5 p) dV, \quad (3)$$

where p , ρ , and v are the pressure, density, and velocity of the gas, and the integration is over the volume V of the shocked gas. We note that, for a nonrelativistic gas, the strong shock jump conditions yield

$$\rho(R_s) = 4\rho_A(R_s), \quad (4)$$

$$v(R_s) = \frac{3}{4}v_{sf}, \quad (5)$$

$$p(R_s) = \frac{3}{4}\rho_A(R_s)v_{sf}^2, \quad (6a)$$

$$T(R_s) = 14 [v_{sf} (\text{km s}^{-1})]^2 \text{ K}. \quad (6b)$$

The quantities on the left-hand side refer to the postshock parameters. Equation (6b) follows from equations (4) and (6a), where a primordial composition of H and He has been assumed. It is evident from these relations that just behind the shock front the kinetic and thermal energies of the gas are partitioned equally: $1/2 \rho(R_s)v^2(R_s) = 3/2 p(R_s)$. As described by Parker (1963, p. 98), the surface of the wave does $p dV$ work and imparts an energy dE to the fluid: $dE = -p dV$. The wave loses energy at a rate dW/dt which is equal to dE/dt . Hence, the total energy in and expended by the wave is $\int dW = -\int dE = \int p dV = \int A_s p(R_s)(dR_s/dt)dt = \int 0.75\rho_A(R_s)v_{sf}^2 A_s dR_s$ where the relation given by equation (6a) has been used. So,

$$W = \frac{3}{4} \int v_{sf}^2 dM, \quad (7)$$

where dM is given by equation (2). Equation (7) suggests that the energy in the wave be written $W = \epsilon M v_{sf}^2$, where ϵ is a fraction of order unity which may be obtained once v_{sf} has been determined from equation (8) (Hundhausen 1985). It can be seen that

$$v_{sf}^2 = \frac{W}{\epsilon M}, \quad (8)$$

where M is obtained by integrating equation (2). W , the total energy in the wave, determines whether a shock wave forms, and, if a shock wave forms, the time dependence of W , (dW/dt) or $W(t)$, determines the type of shock wave which forms. The shock wave types of relevance to the model described above are the driven shock wave and the blast wave. It is assumed that the power emanating from the central source and being collimated through the jets is constant in time, and energy losses due to cooling of the plasma within the jet are neglected. In this case, $W = Pt$, where P is the power emanating from the central source and being collimated down the jets; this will lead to the cylindrically symmetric driven shock wave which will cause the jet to "tunnel" through the ambient gas. The jump discontinuity in the pressure between the outer shock and the adjacent ambient gas (boundary 2 in Fig. 1) corresponds to an impulsive energy input; hence the energy in the shock wave is constant leading to the formation of a blast wave. Given that $\rho_A(R_s)$ and A_s are known, equation (2) may be solved for M . Then equation (8) may be solved to determine the velocity of the shock front v_s for the case of a driven shock wave ($W = Pt$) and the velocity of the shock front v_{bw} for the case of a blast wave ($W = \text{constant}$). We first consider the driven shock wave and then the blast wave. The energy lost by the driven wave to the blast wave is neglected. As discussed below, this is expected to cause the velocity of the forward shock front to be decreased by a factor which is, at most, 0.7 (see the discussion following eqs. [12] and [13]).

In order to obtain the parameters describing the driven

shock wave tunneling through the ambient gas, a density distribution for the ambient gas must be assumed. We shall assume that the matter in the collimated jet has a gas pressure (in the rest frame of the jet fluid) that is greater than or equal to that of the external medium, so that the jet maintains a constant, nonzero opening angle, and that the external medium is isothermal and hence has an r^{-2} density profile, where r is the radial distance from the central, compact source. Then $A_s \propto r^2$ and $\rho_A(r) \propto r^{-2}$, so $A_s \rho_A(r) = \text{constant} = \rho_A(z_0) \pi a_j^2(z_0)$, where z_0 is some fiducial radial coordinate along the symmetry axis of the jet, $2a_j(z_0)$ is the cross sectional diameter of the jet at z_0 , and $\rho_A(z_0)$ is the density of the ambient gas at the distance z_0 from the central compact source; note that an identical result obtains when the jet has a zero opening angle and the medium is of constant density. Integration of equation (2) yields $M = \rho_A(z_0) \pi a_j^2(z_0) R_s$. The energy of the shock wave W is $W = Pt$; hence equation (8) implies that

$$v_s^2 = \frac{Pt}{\epsilon \rho_A(z_0) \pi a_j^2(z_0) R_s} = k \left(\frac{t}{R_s} \right), \quad (9)$$

where $k \equiv P/[\epsilon \rho_A(z_0) \pi a_j^2(z_0)]$. Since $v_s = dR_s/dt$, equation (9) may be integrated to obtain R_s : $R_s = k^{1/3}(t - t_i) + R_s(t_i)$. That is, the velocity of the shock front is constant:

$$v_s = k^{1/3} = \left[\frac{P}{\epsilon \rho_A(z_0) \pi a_j^2(z_0)} \right]^{1/3}. \quad (10)$$

The interaction of the collimated driver wind with the ambient gas causes a driven shock wave to be established, as illustrated in Figure 1. Because the driver wind is assumed to be moving supersonically (relative to both the ambient medium and the jet plasma), this shock wave has a double shock structure: the outer shock contains the shocked ambient gas, the inner shock contains the shocked driver wind, and the two regions are separated by a contact discontinuity. The pressure discontinuity between the gas in the outer shock and the adjacent ambient gas causes a blast wave to propagate into the ambient gas. In the rest frame of the forward shock front, this blast wave will be directed perpendicular to the symmetry axis of the jet. Note that in the rest frame of the central compact object only the postshock material which was in the outer shock has a velocity component parallel to the jet axis. The density along the trajectory of the blast wave should be roughly constant for either a constant density medium or a medium with a radial density gradient if the blast wave propagates a distance S from the symmetry axis of the jet such that $S \ll z_i$ where z_i is the position along the jet at which the blast wave originates. The density along the blast-wave trajectory is $\simeq \rho_A(z_i)$. The area of the shock front is roughly $A_s \simeq 2\pi l S$, where S is the distance of the shock front from the symmetry axis of the jet (see Fig. 2) and l is the thickness of the outer shock front. Equation (2) implies that $M \simeq \pi l \rho_A(z_i) [S^2 - a_j^2(z_i)] \simeq \pi l \rho_A(z_i) S^2$. Equation (8) implies

$$v_{bw}^2 = \left[\frac{W}{\epsilon \pi l \rho_A(z_i) S^2} \right] = \frac{k_{bw}}{S^2}, \quad (11)$$

where $k_{bw} \equiv W/[\epsilon \pi l \rho_A(z_i)]$. Equation (11) may be integrated (note that $v_{bw} = dS/dt$): $S \propto t^{1/2}$, so $v_{bw} \propto t^{-1/2}$, or

$$v_{bw}(t) = v_{bw}(t_i) \left(\frac{t}{t_i} \right)^{-1/2} = v_{bw}(S_i) \left(\frac{S}{S_i} \right)^{-1}, \quad (12)$$

where v_{bw} is the velocity of the blast wave and $v_{bw}(t_i)$ is the

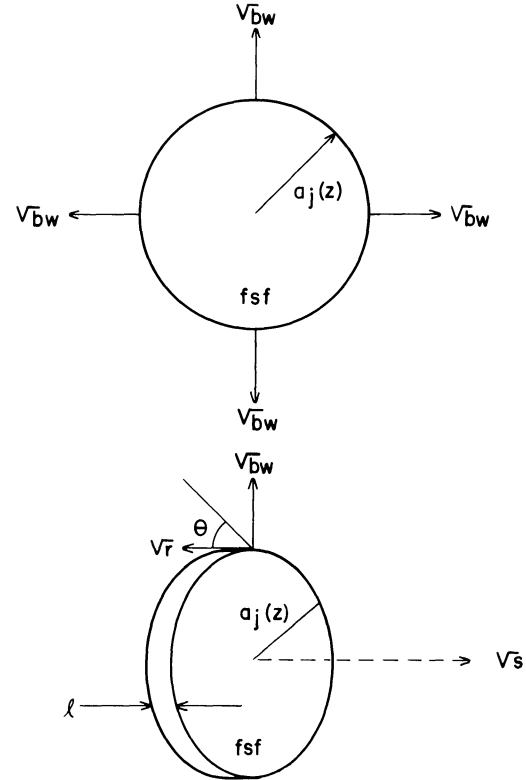


FIG. 2.—The forward shock front (fsf) and the outer shock viewed along the symmetry axis of the jet. The radius of the outer shock is $a_j(z)$, and the thickness of the outer shock is l . The forward shock front moves with a velocity v_s . The blast wave propagates with a velocity v_{bw} . In the rest frame of the forward shock front, the gas in the outer shock has a (relative) velocity v .

initial velocity of the blast wave. The initial velocity of the blast wave, $v_{bw}(t_i)$ may be estimated using Euler's equation: $\partial v/\partial t + v \cdot \nabla v = -(1/\rho) \nabla p$ which, when greatly simplified, implies that $v_{bw}(t_i) \sim (p_{fsf}/\rho_{fsf})^{1/2}$, where p_{fsf} and ρ_{fsf} are the gas pressure and density in the forward shock front. This relation and those expressed in equations (4), (5), and (6a) imply that $v_{bw}^2(t_i) \sim 3/16 v_s^2 \sim 0.2 v_s^2$. Naively, about half the energy is expected to be channeled into the blast wave, and hence about one-quarter is expected to go into shock heating the ambient gas adjacent to the jet. This is because about half the energy input from the jet plasma goes into accelerating and the other half goes into shock heating the gas behind the forward shock front (see the discussion following eqs. [6a] and [6b]). The pressure gradient resulting from the pressure or energy density of the shock heated gas in the outer shock drives the blast wave; hence, most of the energy associated with the pressure of the shock heated gas behind the forward shock front is channeled into the blast wave: since the mass densities just behind the forward shock front and behind the forming blast wave are equal $v_{bw}^2(t_i) \sim 0.5 v_s^2$. Hence, $v_{bw}(t_i)^2$ should fall in the range (0.2 to 0.5) v_s^2 . Equation (12) then implies

$$v_{bw} = (0.4 \text{ to } 0.7) v_s \left(\frac{S}{S_i} \right)^{-1}. \quad (13)$$

Note that this implies that the velocity v_s of the forward shock front is decreased by a factor of 0.9 to 0.7. This factor is not included in subsequent discussions of the velocity of the forward shock front.

The shock envelope is described by the angle θ between the envelope and the z axis (the symmetry axis of the jet) and the position S of the blast wave as a function of distance along the jet, z_i (see Fig. 1). The angle θ is given by: $\tan \theta = v_{bw}/v_s \simeq 0.55 (a_j/S) \simeq 0.55(t_i/t)^{1/2}$. The maximum value of θ , θ_{\max} , is $\theta_{\max} \simeq 30^\circ$; as the blast wave propagates away from the jet axis, θ decreases.

The pressure gradient across boundary 3 (see Fig. 1) will cause material to flow from the inner shock into the shocked gas adjacent to the jet; this region is referred to as the cocoon. The pressure in the inner shock near the contact discontinuity is close to that behind the forward shock front, since the forward shock front will remain very thin and since pressure equilibrium is maintained across the contact discontinuity. The pressure in the inner shock near the contact discontinuity is $P_i \simeq 0.75\rho_A v_s^2$. The pressure in the region adjacent to the jet is given by the pressure just behind the blast wave $P_{bw} \simeq 0.75\rho_A v_{bw}^2$ (see eq. [6a]). Since the velocity of the blast wave is less than that of the forward shock front, the pressure P_i exceeds the pressure P_{bw} , which will cause material to flow into the cocoon. A greatly simplified version of Euler's equation may be used to estimate the velocity, v_i , at which material flows from the inner shock into the adjacent shocked material: $\rho_i v_i (0.75v_{bw} - v_i) = (P_i - P_{bw})$, where ρ_i is the density of material in the inner shock, and $0.75 v_{bw}$ is the velocity of the postshock material in the cocoon (see eq. [5]). Solving this equation, $v_i/v_{bw} = 3/8(1 \pm k)$, where $k = \{1 - 16\rho_A/(3\rho_i)[(v_s/v_{bw})^2 - 1]\}^{1/2}$ is obtained. Hence, v_i must be less than $0.75v_{bw}$, that is, less than $\sim 0.4v_s$ (see eq. [13]). The jet material is most likely magnetized and will carry a magnetic field into the galactic medium when the jet material flows from the inner shock into the cocoon; this could be a source of galactic magnetic fields, as discussed by Daly and Loeb (1989).

IV. DISCUSSION

The approximate analytic expressions obtained in the previous section may be used to estimate the expected properties of a galaxy or protogalaxy possessing a central compact source ejecting material supersonically along two well-collimated jets. The application of these expressions is expected to yield order of magnitude estimates, due to the various assumptions adopted, such as the assumed density profile for the ambient medium.

The interpretation of the alignment effect as the result of star formation triggered by the passage of the jet is only viable if the rotation of the system is negligible, otherwise the elongation axis of the optical emission need not be aligned with that defined by the positions of the radio lobes. The fact that jets are often observed to be straight indicates that the plasma is flowing along a stationary axis, such as the angular momentum axis of the central compact object (presumably a black hole). The angular momentum axis of the galactic/protogalactic gas may or may not be related to that of the central compact object. If the two are not strongly aligned, then the alignment effect indicates that rotation is negligible, which may be taken as a constraint on the minimum velocity of the forward shock front as discussed in § IVa.

The power channeled into the jets may be related to the extent of the blast-wave envelope (which bounds the region within which the star formation may be triggered and the gas shock heated by the passage of the blast wave), since both are related to the velocity of the forward shock front. The relation

between the power channeled into the jets and the velocity of the forward shock front is presented in § IVb, and the extent of the blast-wave envelope is discussed in § IVc.

An important issue is whether star formation is triggered as a result of the jets tunneling through the ambient protogalactic/galactic medium. The conditions expected to lead to star formation, including cooling rates of the shock-heated gas, are discussed in § IVd.

The relative positions of the region of radio emission, optical and infrared emission, and line emission are discussed in § IVe.

The time scale for which the alignment persists, and the implications for the epoch(s) of galaxy formation, are discussed in § IVf.

Much of the shock-heated gas may become unbound from the protogalaxy/galaxy; the effect of such an occurrence on the surrounding medium is discussed in § IVg.

a) Time Scales: The Tunneling Phase and Galactic Rotation

It is important to note that galactic rotation may be neglected while the jets are tunneling through the galactic medium if the velocity of the forward shock front is $\gtrsim 5 \times 10^3$ km s⁻¹, or if the systems possess little angular momentum, or if the angular momentum axis of the galactic/protogalactic ambient medium is aligned with the jet axis. A typical time scale for galactic rotation t_{rot} is $t_{\text{rot}} \simeq 2\pi R/v_{\text{rot}} \simeq 2.5 \times 10^7 (R/\text{kpc})(v_{\text{rot}}/250 \text{ km s}^{-1})^{-1}$ yr, where R is the radial distance from the galactic center and v_{rot} is the circular velocity of the gas about the galactic center. The time scale for the jet to tunnel through the galactic medium is $t_{\text{jet}} \simeq R_g/v_s \simeq 10^6 (R_g/10 \text{ kpc})(v_s/10^4 \text{ km s}^{-1})^{-1}$ yr, where R_g is the radial extent of the galaxy at the time the tunneling occurs. R_g is scaled to 10 kpc; of course, R_g may be significantly larger than 10 kpc. Rotation in the inner regions of the galaxy will require the jets to tunnel through fresh material. New material may move into the line of the jets in a small fraction of a rotation period; hence, the time scale required before rotation becomes important should perhaps be taken to be $t_{\text{rot}} \sim 10^6$ to 10^7 yr. The radio lobes in the radio-selected objects which display evidence for a recent tunneling event are typically separated by less than 1 to 5×10^2 kpc, indicating that the jets have been active for a time $\lesssim 0.5$ to $2.5 \times 10^7 (v_s/10^4 \text{ km s}^{-1})^{-1}$ yr. Hence, galactic rotation may be neglected in these objects if the velocity of the forward shock front is $\gtrsim 5 \times 10^3$ km s⁻¹. If the jets are active for an extended period of time, $t_{\text{jet}} \gtrsim \text{few} \times 10^7$ yr, a new channel through the galactic medium will be carved by the jets unless the medium through which the jets are tunneling possesses little angular momentum; similarly, if the jets are reactivated at a later time, a new channel through the ambient medium will be carved by the jets.

b) The Power of the Central Source and the Shock Velocity

Equation (10) indicates the relation between the velocity of the forward shock front, v_s , and the power channeled down the jets by the central object, P . Given that v_s is constant, ϵ may be determined from equation (7) and is found to be $\epsilon \simeq 9/16 \simeq 0.75$. Choosing some typical numbers for the ambient gas density and width of the jet, equation (10) implies

$$v_s \simeq 10^4 \text{ km s}^{-1} \left[\frac{P}{10^{46} \text{ ergs s}^{-1}} \frac{1 \text{ cm}^{-3}}{n} \left(\frac{0.5 \text{ kpc}}{a_j} \right)^2 \right]^{1/3}, \quad (14)$$

where n is the ambient number density of protons and electrons at the position along the jet where the cross sectional diameter of the jet is $2a_j$. As is evident from equation (14), the

velocity of the forward shock front is fairly insensitive to variations in parameters.

The power P being channeled into the jets may be related to the mass of the central compact object if the compact object is radiating near the Eddington luminosity. The Eddington luminosity is a canonical or reference luminosity; radiation and plasma channeled away from a central compact object over a small solid angle may have a luminosity greater than Eddington, but the Eddington luminosity still provides a good zeroth order estimate. For a power being channeled into the jets of $\sim 10^{46}$ ergs s^{-1} , the mass of the central compact object is $\sim 10^8 M_\odot$, if power is being channeled into the jets at the Eddington luminosity. If the velocity of the forward shock front, the number density in the vicinity of the forward shock front, and the jet radius at that position may be inferred from observations, then the power being channeled into the jets may be estimated from equation (14), and the mass of the central compact object may be estimated if it is assumed that the central compact object is radiating near the Eddington luminosity.

As indicated by equation (13), the initial velocity of the blast wave is about half the velocity of the forward shock front (at the location at which the blast wave originates) and decreases inversely with perpendicular distance from the jet axis. Hence, observations of the velocity field along and perpendicular to the jet axis may be related to the power being channeled into the jets, the ambient density, and the jet radius, via equations (13) and (14); this is discussed in more detail in § IVe.

c) The Extent of the Blast-Wave Envelope

The position of the blast wave at time t in the direction perpendicular to the jet axis $S(t)$ relative to the jet radius at which the blast wave originated $S_i = S(t_i)$ is given by $S = S_i(t/t_i)^{1/2}$ (eq. [12]). Before the forward shock front encounters the intergalactic medium, the velocity of the forward shock front is roughly constant in time for the assumed density profile (see § III). Hence, if the blast wave originates at a position along the jet axis z_i at time t_i , and at time t the forward shock front is at the position z , where $z = R_s$, then $S = S_i(z/z_i)^{1/2}$, since $R_s/t = z_i/t_i$. This relation is valid until the velocity of the blast wave becomes comparable to the sound speed of the ambient gas; this occurs at the position S_{\max} , at a time $t/t_i \approx 0.35 v_s^2/c_s^2$, which yields ages consistent with the results of Chambers and Charlot (1990).

The blast-wave envelope is defined by the position S_{\max} , the perpendicular distance from the jet axis at which the blast wave deteriorates into a sound wave. This occurs when the velocity of the blast is on the order of the sound speed of the medium. The sound speed for a medium of primordial composition of H and He at a temperature T_A is $c_s \approx 300 \text{ km s}^{-1}$ ($T_A/4 \times 10^6 \text{ K}$) $^{1/2}$; note that the virial temperature of a $10^{12} M_\odot$ object with a virial radius of 50 kpc is $\approx 4 \times 10^6 \text{ K}$. The velocity of the blast wave is given by equation (13). Hence,

$$S_{\max} \approx 18 \left(\frac{v_s}{10^4 \text{ km s}^{-1}} \right) \left(\frac{T_A}{4 \times 10^6 \text{ K}} \right)^{-1/2} a_f(z_i), \quad (15)$$

where $a_f(z_i)$ is the radius of the jet at the position at which the blast wave forms (see eq. [9]).

The emission from the stars whose formation is triggered by the passage of the blast wave must arise from within the shock envelope. Immediately after the passage of the shock wave, line and continuum emission from the shock-heated gas also arises

from within the shock envelope. Later, however, the shock-heated gas may escape from the galaxy, as discussed in § IVg.

The mass of the shock-heated gas may be estimated. If the region is approximated as a cylinder of radius S_{\max} and length R_g , with an average number density of protons and electrons n , the mass of the shock-heated gas is $M \sim 10^{11} M_\odot (n/0.1 \text{ cm}^{-3}) (S_{\max}/18 \text{ kpc})^2 (R_g/100 \text{ kpc})$.

d) Cooling and Star Formation

The shock-heated gas is expected to cool via bremsstrahlung emission, line emission, and Compton cooling (which is effective at very high redshifts [$z \gtrsim 7$] due to the increase in the number density of the photons comprising the relic radiation and may be effective at lower redshifts if there is a soft photon field). The relativistic electrons in the jet and in the radio lobes cool via synchrotron emission and by Compton cooling. Cooling will be important if the cooling time scale is less than the other relevant time scales in the problem.

Cooling may be important behind the shock front of the driven shock wave or behind the shock front of the blast wave. It is interesting to note that there is only a very small range of forward shock velocities for which *both* cooling behind the driven shock wave is not important, *and* cooling immediately adjacent to the jet, behind the blast wave, is important. Except for this small range of parameters, cooling behind the forward shock front is always important if it is important behind the blast wave in the immediate vicinity of the jet (although cooling further away from the jet may be important for a wide range of parameters, as discussed below). However, if cooling is important behind the forward shock front, the blast wave will not form. This means that star formation in the region adjacent to the jet may only occur as a result of cooling behind the blast wave for a very special range of parameters, as described below. Alternatively, star formation may occur in this region if the ambient medium consists of cold clouds embedded in a hot medium, since the passage of the shock wave will trigger star formation in the cold clouds, as discussed in detail by Rees (1989).

When the temperature of the shock-heated gas exceeds about 10^6 K , which will be the case when the velocity of the forward shock front is greater than about 250 km s^{-1} , the primary cooling mechanism will be thermal bremsstrahlung emission. The time scale for the gas to cool via this mechanism is $t_{\text{cool, tb}} \sim E/L$, where E is the thermal energy of the gas, $E = nkTV$, L is the total luminosity emitted by thermal bremsstrahlung radiation, and V is the volume occupied by the gas. The luminosity L is $L = 1.4 \times 10^{-27} T^{1/2} n_e n_p Z^2 g_B c_L V$ ergs s^{-1} (e.g., Rybicki and Lightman 1979). Hence, $t_{\text{cool, tb}} \sim 1.6 \times 10^3 T^{1/2} (\text{K})/[n(\text{cm}^{-3})c_L] \text{ yr} = 6 \times 10^3 v_{\text{sf}} (\text{km s}^{-1})/[c_L n(\text{cm}^{-3})] \text{ yr}$, where v_{sf} is the velocity of the shock front obtained from the temperature using equation (6b), c_L is the clumping factor given by $c_L = \langle n^2 \rangle / \langle n \rangle^2$, and the metallicity times the gaunt factor $Z^2 g_B$ has been taken to be ~ 2 relevant for a plasma of primordial composition; increases in metallicity will increase this factor and decrease the cooling time.

If the time scale for the gas to expand, t_{exp} , is less than that for radiative cooling, adiabatic cooling behind the shock front will dominate, and the calculations presented in § III remain unchanged. In this case, star formation will not occur as a result of cooling behind the shock front. The expansion occurs in the direction along the steepest pressure gradient which, in this model, is in the direction perpendicular to the jet axis. Hence, the expansion time scale is $t_{\text{exp}} \sim S/c_s$, where S is the

characteristic size of the region which has been shock heated and c_s is the sound speed of the gas in this region. Since the sound speed depends only on the temperature of the shock-heated gas, which may be related to the velocity of the shock front (see eq. [6b]), $t_{\text{exp}} \sim 1.8 \times 10^9 S(\text{kpc})/v_{\text{sf}}(\text{km s}^{-1}) \text{ yr}$.

Behind a shock front, cooling via thermal bremsstrahlung emission may be neglected when $t_{\text{exp}} < t_{\text{cool, tb}}$, that is, when the velocity of the shock front satisfies

$$v_{\text{sf}} > 0.5 \times 10^3 \text{ km s}^{-1} [S(\text{kpc})n(\text{cm}^{-3})c_L]^{1/2}, \quad (16)$$

where S is the characteristic size of the shock-heated region along the direction of the steepest pressure gradient which will expand behind the shock front, n is the number density of electrons in the shock-heated region, and c_L is the clumping factor defined above; the symbol v_{sf} has been used to stress that this expression is applicable to any shock system.

Cooling behind the forward shock front will be negligible when

$$v_s > 0.5 \times 10^3 \text{ km s}^{-1} (a_j n c_L)^{1/2}, \quad (17a)$$

where a_j is the jet radius in kpc, and n is the electron number density of the shock-heated gas in cm^{-3} .

Equation (16) applied to the blast wave yields

$$v_{\text{bw}}(t_i) > 0.5 \times 10^3 \text{ km s}^{-1} (S/a_j)(S n c_L)^{1/2}, \quad (17b)$$

since $v_{\text{bw}} = v_{\text{bw}}(t_i)(S/a_j)^{-1}$; S is in kpc.

The cooling time in the region immediately adjacent to the jet, given by equation (17b), may be directly compared to that just behind the driven shock wave, given by equation (17a), by using the relation between the two shock front velocities given in equation (13): $v_{\text{bw}}(t_i) \simeq 0.55v_s$. Hence equation (17b) indicates that cooling in the region adjacent to the jet will be important for $v_s < 10^3(S/a_j)(S n c_L)^{1/2}$, where v_s , S , a_j , and n have the units indicated above. Scaling the perpendicular distance from the jet axis to the jet radius, $S = \alpha a_j$, equations (17a) and (17b) indicate that cooling will not be important behind the forward shock front, but will be important behind the blast wave, at the distance αa_j from the jet axis when

$$1 < \left[\frac{v_s}{5 \times 10^2 (a_j n c_L)^{1/2}} \right] < 2\alpha^{1.5}, \quad (18)$$

where v_s is in km s^{-1} . Suppose the blast wave has propagated one scale length from the jet axis; then $\alpha = 2$, and the upper limit indicated in equation (18) becomes about 6. This shows that there is only a small range of parameters for which cooling behind the forward shock front will be negligible, but cooling immediately adjacent to the jet, behind the blast wave, will be important. As α increases, cooling may become important; however, as α increases, the postshock conditions become more similar to the preshock conditions, so it is difficult to see how the passage of the shock wave could trigger star formation.

The results obtained above are applicable for either a jet with a zero opening angle interacting with a constant density medium (the case studied numerically by De Young 1989), or for a jet with a constant nonzero opening angle interacting with a medium possessing the density profile characteristic of an isothermal sphere (see the discussion preceding eq. [9]). Hence, these results can be compared with those obtained numerically by De Young (1989); see also De Young (1986) and Norman, Winkler, and Smarr (1983). He chose the following parameters: $n = 10$ (indicating an initial postshock density

of 40), $c_L = 1$, and $a_j = 0.6$. Substituting these numbers into equation (18), the limit on the velocity of the forward shock front becomes:

$$1 < \left(\frac{v_s}{2 \times 10^3} \right) < 6 \left(\frac{\alpha}{2} \right)^{1.5}. \quad (19)$$

If the cooling is to occur within a cylinder about the jet which extends one jet radius from the jet, then α must be less than 2. The velocity of the forward shock front used in the numerical simulations may be deduced from the on-axis temperature range of $0.3\text{--}2 \times 10^8 \text{ K}$ quoted (De Young 1989): $v_s = 1.5\text{--}4 \times 10^3 \text{ km s}^{-1}$; the velocity deduced in this way agrees with that determined from the quoted velocity of the material within the jet, $1\text{--}3 \times 10^3 \text{ km s}^{-1}$, since the velocity of the material within the jet is expected to be $\sim 0.75v_s$ (see eq. [5]). Equation (19) indicates that this falls into just the range of velocities of the forward shock front for which we expect cooling to be important in the region immediately adjacent to the jet, but not behind the forward shock front (which would prevent the formation of the blast wave). The cooling time scale estimated above was $t_{\text{cool, tb}} \simeq 6 \times 10^3 v_{\text{sf}}/(n c_L) \text{ yr} \simeq 1.5\text{--}4.5 \times 10^5 \text{ yr}$ for the parameters chosen by De Young (1989); this is to be compared to the values he obtained numerically: between 10^5 and 10^6 yr . It is a gratifying test of the analytic calculations presented here and in § III that our results agree so well with the results of the numerical simulations.

As is evident from equation (17b), when the velocity of the forward shock front is increased, the region in which cooling becomes important moves away from the immediate vicinity of the jet, farther from the jet axis; similarly, if the ambient number density or jet radius differ from the values chosen, cooling behind the blast wave will not be important.

There will be many combinations of parameters for which cooling behind the shock fronts will not be important. Star formation in these systems may still occur if the ambient medium is initially in two phases. As discussed by Rees (1989), in this case the shock front bypasses the cold clouds, which subsequently collapse in the high-pressure environment of the shock-heated gas. In this case, the stars and shock-heated gas should lie within the shock envelope (discussed in § IVc).

Chambers and McCarthy (1989) demonstrate that star formation is a mandatory component of any model to explain the alignment effect.

e) *The Relation between the Emitting Regions*

Three primary sources of emission may be identified: the radio emission from the radio lobes and hot spots, the optical (and infrared) emission from the stars, and free-free and line emission from the gas, which in addition to being collisionally excited may be excited by the stellar radiation field (see, for example, Djorgovski and Spinrad 1984a), or by UV emission from the central compact source (van Breugel and McCarthy 1990). The line ratios presented and discussed by van Breugel and McCarthy (1990) indicate that the UV emission from the central compact source is exciting the O II line emission. This would lead to an alignment of the O II emission region with the jet axis if the optical depth in the jets is much less than that exterior to the jets in the vicinity of the central compact source, so that at large distances from the central compact source, only the O II in the vicinity of the jet would be excited by the UV emission from the central compact source.

It is instructive to consider the relative volumes occupied by

each of these components neglecting radiative cooling. Assuming cylindrical symmetry about the jet axis, the relative volumes occupied may be determined by the extent of the blast-wave envelope S_{\max} (discussed in § IVc) relative to the separation between the forward shock fronts of the oppositely directed jets (R_{r1}). The emission from the stars and shock-heated gas is expected to arise from the same region; in addition, regions in which cool gas is entrained in the hot medium will be strong emission-line regions, and these may coincide with the regions in which star formation has not been efficient, since the high-density regions which were heated so that star formation did not occur will be able to cool efficiently and hence can cool to temperatures where line emission is important. The fact that the O II lines exhibit the large velocity gradients typical of the hot postshock gas indicates that this cooler, line-emitting gas is entrained in the hot, high-velocity medium. And, as noted above, if the optical depth within the jet is small compared to that outside the jet, the O II emission will be excited by the UV emission from the central compact source in a region which is elongated along the jet axis.

The radio emission is inferred to be synchrotron emission and hence indicates the presence of relativistic electrons and a magnetic field (on the observational side; see Djorgovski *et al.* 1987). The radio lobes and hot spots are identified with the inner shock of the driven shock wave, because this region contains the shocked jet material which very likely contains a magnetic field. Hence, the relative regions of the optical, infrared, and line emission and of the radio emission result from a comparison of S_{\max} (the maximum extent of the shock envelope in the direction perpendicular to the jet axis) and R_{r1} (the separation between the radio lobes or hot spots).

Combining equation (15) with $R_{r1} = 2v_s t_{\text{jet}}$, where t_{jet} is the time for which the jet has been active and v_s is the average velocity of the forward shock front, we find $S_{\max}/R_{r1} \approx [a_j(z_i)/\text{kpc}](t_{\text{jet}}/10^6 \text{ yr})^{-1}$, for $T_A = 4 \times 10^6 \text{ K}$; note that this expression is independent of v_s ; if the ratio S_{\max}/R_{r1} and the typical jet radius may be determined from the observations, the time t_{jet} may be deduced, and this time and the distance R_{r1} may be used to infer the typical velocity of the forward shock front (if radiative cooling has been negligible, as it will be under most circumstances: see § IVd). In the case of 3C 368 (Djorgovski *et al.* 1987; Chambers, Miley, and Joyce 1988), observations indicate that $S_{\max}/R_{r1} \lesssim 1/4$. Let the value of S_{\max}/R_{r1} be $\approx x/4$, where $x \lesssim 1$. Then $t_{\text{jet}} \sim 4 \times 10^6 x^{-1} (a_j/\text{kpc}) \text{ yr}$. For a Hubble constant of $50 \text{ km s}^{-1} \text{ Mpc}^{-1}$ and deceleration parameter $q_0 = 0.5$, the observed separation of the radio lobes is about 70 kpc, which is $\sim 2v_s t_{\text{jet}}$. Combining these two equations, the velocity of the forward shock front must satisfy $v_s \sim x \times 10^4 \text{ km s}^{-1} (a_j/\text{kpc})^{-1}$, where $x \lesssim 1$.

Alternatively, the velocity of the forward shock front, v_s , may be inferred from the observed separation of the radio lobes and from the inferred age of the stars whose formation is triggered by the passage of the jets, since t_{jet} should be \sim the age of the stars; in addition, the observed velocity gradient along the jet axis will yield an estimate of the current velocity $2v_s$; note that this velocity could have been significantly smaller in the past if the jets are currently interacting with the intergalactic medium which has a much lower density than the ambient medium of the galaxy (see eq. [14]). Similarly, the velocity gradient perpendicular to the jet axis yields an estimate of $2v_{\text{pw}}$; a systematic variation of the velocity perpendicular to the jet axis as a function of position along the jet axis could be used to infer the history of the velocity v_s , that is, to deduce how constant v_s has been.

If the stars in 3C 368 are $\sim 3 \times 10^8 \text{ yr}$ old, as suggested by Chambers and Charlot (1990), then the average velocity of the forward shock front over that $3 \times 10^8 \text{ yr}$ is $\sim 100 \text{ km s}^{-1}$, which seems fairly small. Such a low velocity may indicate that cooling was important behind the forward shock front. In this case, the mean velocity of the forward shock front is decreased from that determined in § III (where cooling was neglected), and from its current velocity if cooling behind the forward shock front was important in the past but is no longer important as a result of the decrease in the ambient density. While radiative cooling is important behind the forward shock front, much of the energy channeled into the jets is lost to thermal bremsstrahlung emission (see § IVd). In fact, the X-ray emission resulting from this cooling may contribute to the high-energy X-ray background (Daly, 1990). Alternatively, the jets may be carving a new channel, in which case the age estimates given in § IVc are applicable.

f) Implications for the Epoch(s) of Galaxy Formation

The observations of these galaxies are relevant to the epoch(s) of galaxy formation in two ways. First, the alignment of the infrared component (e.g., 3C 368 [Chambers, Miley, and Joyce 1988]) suggests that this component is related to the jets and hence might be expected to be fairly young. Not only is the red (assumed stellar) component observed in the K band aligned with the radio axis, as is the blue component, but it seems to be spatially coincident with the blue component and with the line-emitting region, both of which terminate at the radio lobes, at least in the case of 3C 368 (Chambers, Miley, and Joyce 1988); the infrared emitting region may be very slightly less extended than the line-emitting and the higher energy continuum emission regions along the jet axis in 3C 368, but this is within the noise. On the other hand, the infrared Hubble diagram for the complete 3C and 1 Jy radio galaxies argues that the red stellar component is quite old, as discussed in detail by Lilly and Longair (1984) and by Lilly (1989). If the red component is young, there is no apparent reason why galaxies exhibiting the alignment effect (which generally also have relatively high star formation rates) should fall on the same line on the infrared Hubble diagram as high-redshift radio galaxies in which the red component is inferred to be old: those that do not exhibit the alignment effect and that do not have high star formation rates as measured by Lilly's (1989) f_{5000} parameter; however, see Chambers and Charlot (1990).

Suppose that the red component is quite old. This component could exhibit the alignment effect if the jets were active in the past (about 10^9 yr prior to the current age of the system) and triggered star formation, and the red stars are the aging relics from this event. Two processes which would tend to isotropize the distribution of the stars since their formation are the precession of orbits, and violent relaxation. The latter is expected to occur if the second major active phase of the source (which is leading to the current burst of star formation and the bright radio components) is the result of the infall of a significant amount of matter into the gravitational potential of the galaxy, which will cause the potential to be time variable until a new equilibrium distribution of matter is established, leading to violent relaxation (Lynden-Bell 1967; Shu 1978). Violent relaxation will also result if the tunneling of the jets through the ambient medium causes a significant amount of material to become unbound from the galaxy or significantly perturbs the gravitational potential.

In addition, the orbits of the stars will precess; unless the precession angle is close to $n\pi$, precession will cause the aligned

component to be smeared out (unless that component is identified as a disk viewed edge-on). I have investigated the precession of orbits in a logarithmic potential, relevant for the mass distribution of an isothermal sphere. The precession angle ϕ is given by

$$\phi = 2 \int_{x_{\min}}^1 \frac{dx}{x \sqrt{-\beta x^2 \ln(x) + (x^2 - 1)}}, \quad (20)$$

where the initial radial coordinate of the star is R_{\max} , the closest approach to the center of mass of the system is R_{\min} , $x_{\min} = R_{\min}/R_{\max}$, which is related to β by $\beta \ln(x_{\min}) = 1 - x_{\min}^{-2}$, and $\beta = (GM_T/R_v)[v_{\perp}(R_{\max})]^{-2}$, where M_T is the total mass of the system, R_v is the virial radius of the system, and $v_{\perp}(R_{\max})$ is the initial velocity of the star perpendicular to the radius vector originating at the center of mass of the system.

The free parameter in the calculation is β . As mentioned above, equation (20) is a good approximation to the precession angle if the gravitational potential is roughly spherically symmetric and the density distribution may be approximated as $\rho \propto r^{-2}$. Reasonable values for β range from about 10 to 100. In all cases, the precession angle differs from $n\pi$ by at least $\sim 30^\circ$. Exploring values of the parameter from 3 to 300 did not bring the precession angle significantly closer to $n\pi$. It may be concluded that the precession of orbits and/or violent relaxation will smear out the elongated stellar distribution in about one dynamical time of the system. The dynamical time of the system is $t_{\text{dyn}} \sim 3 \times 10^8 (10^{12} M_{\odot}/M)^{0.5} (R_v/50 \text{ kpc})^{1.5} \text{ yr}$. If the system contains about $10^{11} M_{\odot}$ and extends to about 50 kpc, the dynamical time of the system will be about 10^9 yr . If the dynamical time of the system is long enough, the red component could be due to old stars.

If no significant old red population of stars is present in the galaxies exhibiting the alignment effect, then there is no evidence that these are elliptical galaxies, or the precursors to present-day ellipticals. They may in fact be precursors to either present-day spiral or elliptical galaxies. The upper limit on the luminosity of a red component which is roughly spherical in shape could be used to place an upper limit on the mass of an old component in these galaxies, which would be an important constraint on the epoch of the first major burst of star formation in these systems, and hence a hint concerning the epoch of galaxy formation. A tight upper bound on the mass of an old component could be taken as a clue that a violent event is needed to trigger the initial burst of star formation, at least in these systems. These galaxies would then be quite similar to the gas-rich systems observed by Gunn and Dressler (e.g., Gunn 1989).

It may also be possible that the red component seen to be highly elongated may be a small portion of a larger, spherically symmetric distribution of old red stars. Lilly (1989) points out that in the galaxies with high star formation rates, a significant fraction of the light observed in the K band arises from the light associated with the young stars, hence enhancing the observed alignment of the red and blue components. Fainter infrared images of galaxies exhibiting the alignment effect, and the alignment of the red component in galaxies with less star formation activity as measured by Lilly's f_{5000} parameter will allow a determination of the alignment of the red component which is not contributing to the blue continuum.

A second implication for galaxy formation and evolution may be deduced from the observations discussed. The alignment effect exhibited by the steep-spectrum radio sources indi-

cating a recent burst of star formation, and other observations of copious activity over the redshift interval from about 1 to 3 or so, such as the rise and fall in the quasar number counts, and the blue galaxies seen by Tyson (1988), suggest a second important epoch of galaxy formation or evolution. Hence, the observations of the radio galaxies may indicate that there are two major epochs of galaxy evolution, at least for the sources exhibiting the alignment effect. The first occurs early and is indicated by the presence of old elliptical galaxies seen at high redshift. A second major epoch of gas infall onto the old galaxies (and perhaps the formation of some new galaxies, such as 3C 326.1: McCarthy *et al.* 1987a) would occur over the redshift interval from 1 to 3. This would cause the fueling which leads to the activation of the jets in the galaxies exhibiting the alignment effect, and, perhaps, the epoch at which spiral galaxies acquire their disks. Note that these may be two important stages with observational consequences that cause these galaxies to stand out, but the underlying gravitational growth may be continuous, as in a hierarchical model. Two epochs would stand out observationally, for example, if one signals the first major epoch of star formation, and the second signals the first major epoch in the formation of clusters of galaxies.

As discussed by McCarthy *et al.* (1987a), the radio source 3C 326.1 may be an example of a young galaxy. It could be an object in which star formation and shock heating is occurring as jets tunnel through the ambient medium, but which does not have an old red stellar population (McCarthy *et al.* 1987a). Hence, if the red stellar population in such objects as 3C 368 were old, then these would be undergoing refueling which reactivates the jets, whereas 3C 326.1 may have formed recently, and in any case is undergoing star formation and shock heating for the first time. If, on the other hand, the red stellar component of 3C 368 were comprised of young stars, then the initial mass function for the stars whose formation is triggered in 3C 368 must be different from the initial mass function for the stars whose formation is triggered in 3C 326.1.

g) Enrichment of the Environs

The shock-heated gas may have a velocity greater than the escape velocity of the galaxy. This gas may be enriched due to supernova explosions which occur before the gas escapes from the galaxy. It is well known (e.g., Sarazin 1988, and references therein) that the cluster environment contains a mass in gas which is comparable to the gas mass associated with the individual galaxies in the cluster, and is very metal rich, containing at least roughly half the solar abundance heavy elements. If the radio galaxies exhibiting the alignment effect are in a cluster or protocluster, the intracluster medium could be enriched in heavy elements by the gas escaping from the radio galaxies. Radio galaxies with jets which are in a high-density medium, such as a cluster or protocluster of galaxies, will possess bright radio lobes for a longer period of time than similar galaxies in a lower density region, and hence they will have a higher chance of being observed in a radio survey; these galaxies will be preferentially observed. In addition, in a high-density environment there may be more gas available to fuel the compact object, which is the source of the jets. The gas ejected from galaxies in a lower density environment, such as a group of galaxies or an isolated galaxy, may escape from the system altogether.

V. SUMMARY

An interesting and apparently widespread correlation seen in radio sources with steep spectral indices (≥ 1) between

the region of the optical emission and the axes of the radio jets has been observed (Chambers, Miley, and van Breugel 1987, 1988; McCarthy *et al.* 1987*b*). Such a correlation would exist if the continuum and line emission arise from stars and shock-heated gas associated with the tunneling of jets through the ambient medium. The line emission arises from gas near the jet axis and may be radiatively excited by emission from the central compact object (van Breugel and McCarthy 1990), excited by the stellar radiation field, or collisionally excited (see § IVe). The optical emission probably results from the stars whose formation is triggered by the passage of the disturbance (see § IVd), which in turn is driven by the shocks associated with the jets, although free-free emission may contribute to the total observed continuum emission.

Here we consider the shock systems which will form as the material flowing through the jets interacts with the ambient gas associated with these galaxies. The disturbance which propagates into the galactic medium will shock heat the gas and may trigger star formation; whether the gas is shock heated and whether star formation is triggered depend upon the properties of the jet and on the state of the medium prior to the passage of the shocks (see § IVd). The properties of the shock system in relation to the overall properties of the galaxy are discussed (see §§ IVa–IVc). Order of magnitude estimates for the relations between the regions of radio, emission-line, and optical emission are obtained and discussed (see § IVe).

The analysis of the galaxies exhibiting the alignment effect may have important implications for the epoch(s) of galaxy formation, as discussed in § IVf; the length of time for which the alignment will persist is also discussed in that section. Also, galaxies exhibiting the alignment effect may enrich their environs (see § IVg).

The alignment effect between the regions of radio and optical emission may provide insight into how a burst of star formation is triggered in these galaxies. It is possible that such an evolutionary phase in the history of a galaxy is not uncommon. Donnelly, Partridge, and Windhorst (1987) note that the steep-spectrum radio sources, with spectral indices in excess of 1, in their deep VLA fields are unidentified optically, and are probably at redshifts greater than 0.5. Recall that a spectral

index in this range was the selection criterion used by Chambers, Miley, and van Breugel (1987, 1988); most of these galaxies have turned out to be high-redshift galaxies in which the optical emission is aligned with the radio lobes. If the sources observed by Donnelly, Partridge, and Windhorst (1987) are of the same type, then objects exhibiting the alignment effect number at least 50 per square degree (see the discussion in § I).

There are several important consequences if a tunneling phase by jets through the ambient protogalactic/galactic medium is a common stage of galactic evolution: if thermal-bremsstrahlung radiation is the primary cooling mechanism of the shock-heated gas, then the combined emission from these galaxies could contribute significantly to the X-ray background (Daly 1990), the “leakage” of the magnetic field from the jet into the ambient medium could be related to the origin of galactic magnetic fields (Daly and Loeb 1989), and jets could also be a source of heavy elements and magnetic fields in clusters of galaxies.

As more of these “aligned sources” are observed in detail, it will be interesting to note the typical velocity gradients along and across the jet axis, and whether there are systematic differences, such as degree of alignment between the infrared component, the optical component, and the line-emitting regions, relative to the radio lobes.

Note added in manuscript.—Mitchell Begelman and Denis Cioffi (1989) discuss a similar model to explain the alignment effect.

The author would like to thank Jim Peebles for his insightful comments on this work. She would also like to thank Tod Lauer for several pertinent and helpful discussions, and Ken Chambers, Roger Chevalier, Dave De Young, George Djorgovski, Alan Lightman, Simon Lilly, Avi Loeb, Alan Marscher, Patrick McCarthy, George Miley, Bruce Partridge, Martin Rees, Hyron Spinrad, Wil van Breugel, and Jasper Wall for their helpful comments. In addition, an anonymous referee suggested several changes which have substantially improved the paper. This work was supported in part by the National Science Foundation.

REFERENCES

- Begelman, M. C., Blandford, R. D., and Rees, M. J. 1984, *Rev. Mod. Phys.*, **56**, 255.
- Begelman, M. C., and Cioffi, D. 1989, *Ap. J. (Letters)*, **345**, L21.
- Chambers, K. C., and Charlot, S. 1990, *Ap. J. (Letters)*, **348**, L1.
- Chambers, K. C., and McCarthy, P. J. 1989, preprint.
- Chambers, K. C., Miley, G. K., and Joyce, R. R. 1988, *Ap. J. (Letters)*, **329**, L75.
- Chambers, K. C., Miley, G. K., and van Breugel, W. 1987, *Nature*, **329**, 604.
- . 1988, *Ap. J. (Letters)*, **327**, L47.
- Chevalier, R. A., and Imamura, J. N. 1983, *Ap. J.*, **270**, 554.
- Daly, R. A. 1990, in preparation.
- Daly, R. A., and Loeb, A. 1989, *Ap. J.*, submitted.
- De Young, D. S. 1986, *Ap. J.*, **307**, 62.
- . 1989, *Ap. J. (Letters)*, **342**, L59.
- Djorgovski, S., Spinrad, H., Pedetty, J., Rudnick, L., and Stockton, A. 1987, *A.J.*, **93**, 1307.
- Donnelly, R. H., Partridge, R. B., and Windhorst, R. A. 1987, *Ap. J.*, **321**, 94.
- Gunn, J. E. 1989, in *The Epoch of Galaxy Formation*, ed. C. S. Frenk, R. S. Ellis, T. Shanks, A. F. Heavens, and J. A. Peacock (Dordrecht: Kluwer), p. 167.
- Hundhausen, A. J. 1985, in *Collisionless Shocks in the Heliosphere; a Tutorial Review*, ed. R. G. Stone and B. T. Tsurwtau (Washington, DC: American Geophysical Union), p. 37.
- Le Fèvre, O., and Hammer, F. 1988, *Ap. J. (Letters)*, **333**, L37.
- Lilly, S. J. 1988, *Ap. J.*, **333**, 161.
- . 1989, *Ap. J.*, **340**, 77.
- Lilly, S. J., and Longair, M. S. 1984, *M.N.R.A.S.*, **211**, 833.
- Lynden-Bell, D. 1967, *M.N.R.A.S.*, **136**, 101.
- McCarthy, P. J., Spinrad, H., Djorgovski, S., Strauss, M. A., van Breugel, W., and Liebert, J. 1987*a*, *Ap. J. (Letters)*, **319**, L39.
- McCarthy, P. J., van Breugel, W., Spinrad, H., and Djorgovski, S. 1987*b*, *Ap. J. (Letters)*, **321**, L29.
- Norman, M. L., Winkler, K. H., and Smarr, L. 1983, in *Astrophysical Jets*, ed. A. Ferrari and A. G. Pacholezyk (Dordrecht: Reidel), p. 227.
- Parker, E. N. 1963, *Interplanetary Dynamical Processes* (New York: Interscience).
- Rees, M. J. 1989, *M.N.R.A.S.*, **239**, 1P.
- Rybicki, G. B., and Lightman, A. P. 1979, *Radiative Processes in Astrophysics* (New York: Wiley-Interscience).
- Sarazin, C. L. 1988, *X-ray Emissions from Clusters of Galaxies* (Cambridge: Cambridge University Press).
- Shu, F. H. 1978, *Ap. J.*, **225**, 83.
- Spinrad, H. 1986, *Pub. A.S.P.*, **98**, 601, 269.
- Spinrad, H., and Djorgovski, S. 1984*a*, *Ap. J. (Letters)*, **280**, L9.
- . 1984*b*, *Ap. J. (Letters)*, **285**, L49.
- Tyson, J. A. 1988, *A.J.*, **96**, No. 1, 1.
- van Breugel, W. J. M., Heckman, T. M., Miley, G. K., and Filippenko, A. V. 1986, *Ap. J.*, **311**, 58.
- van Breugel, W. J. M., and McCarthy, P. J. 1990, in *Proc. A.S.P. Hubble Symposium*, in press.